J. COMBIN. MATH. COMBIN. COMPUT. 127a (2025) 7923--7945

Journal of Combinatorial Mathematics and Combinatorial Computing
www.combinatorialpress.com/jcmcc

Combinatorial Press

Study on distributed source-load aggregation strategy and capacity optimization considering power supply security constraints in distribution networks

Shiyuan Ni[1], Guilian Wu[1], Sudan Lai[1,✉], Lu Tang[1]

[1] *State Grid Fujian Economic Research Institute, Fuzhou, Fujian, 350012, China*

ABSTRACT

With the rapid development of distribution networks in China and the increasing penetration of renewable and traditional energy sources, it is necessary to study the optimal allocation of capacity and optimal operation for the two stages of pre-planning and practical application of distribution networks. In this paper, the probability density function is used to model the uncertainty of "source" and "load" respectively, and the optimal allocation model of distributed power supply capacity of distribution network system is constructed by the equipment models of "wind generator", "photovoltaic generator", "diesel generator" and "battery". Comprehensive cost and power supply security are taken as the objective function and constraints, respectively, to improve the distributed power supply capacity optimization, and adaptive sparrow search algorithm is applied to solve the model. In the comparative analysis of source-load synergy, source-load synergy and energy storage system joint optimization configuration scheme, the joint planning of DPV and ESS enhances the installed capacity of DPV by about 13.45%, and the average power generation of the joint planning scheme is 88.35 kW/h. The joint planning obviously enhances the installed capacity of DPV under the condition of slightly increasing the DPV curtailment. Examples are examined to verify the practical application of the proposed adaptive sparrow search algorithm in configuring the power supply capacity of the hybrid generation system, and the cost of using the cyclic charging operation scheme is 81,067 yuan lower than that of using the load-tracking scheme, and the economic effect has been significantly improved.

Keywords: probability density function, distributed power capacity optimization, adaptive sparrow search algorithm, source-load coordination

✉ Corresponding author.
E-mail address: HP18721861985@163.com (S. Lai).
Received 12 January 2024; Revised 25 March 2024; Accepted 25 December 2024; Published Online 15 April 2025.
DOI: 10.61091/jcmcc127a-436

1. Introduction

With the proposal of China's dual-carbon goal, the need to accelerate the construction of a new type of power system with new energy as the main body, and to promote the cooperative operation of large-scale distributed source, load and storage resources accessing the power grid has become more and more urgent. Considering the decentralized distribution of massive distributed resources and inconsistency of power output, distributed power, load, and energy storage aggregators can flexibly participate in the interactive regulation and control of the power grid by aggregating various types of distributed resources [1-3]. As the operation of the new power system presents the characteristics of "double high, double peak", which brings great challenges to the safe operation of the system [4]. On the one hand, the high proportion of distributed renewable energy generation leads to the increased difficulty of power balance in the distribution system [5-6]. On the low-voltage distribution side, the temporal and spatial mismatch between renewable energy generation and loads leads to heavy overload and power back-feeding problems in the station area [7]. On the MV distribution side, the stochastic and volatile nature of renewable energy generation causes the problem of dramatic net load creep [8]. On the other hand, a high percentage of distributed power electronic equipment significantly reduces the system moment of inertia, leading to more difficult system frequency regulation [9-10]. For the distribution grid power system, the distributed generation process, the energy storage mode has a certain degree of randomness and volatility, and the irregular penetration of energy sources will cause a certain degree of impact on the stability of the active distribution grid [11-14]. In-depth studies have found that the distributed source-load aggregation strategy has a certain peaking effect, which can optimize electric energy to a large extent and improve the quality and stability of electric energy supply [15-17]. Demand-side to achieve the optimization of the grid and give users a better power service experience, a variety of scheduling methods used to optimize the active distribution network have been proposed to improve the reliability and economy of power supply [18-21]. After the technicians carried out the phase work, they proposed to take into account the security constraints of the grid and the source-load aggregation method during the distribution grid power supply process to achieve the purpose of improving the utilization of electric energy and guaranteeing the stable operation of the grid [22-25].

Microgrids, as one of the basic consumption methods of renewable energy, have received extensive attention and research on the security of their frequency regulation. Zheng, S. et al. developed a distributed power dispatch optimization model considering frequency security constraints and load demand uncertainty, converted the model into a mixed-integer linear programming problem and solved it, so that autonomous microgrids operated with frequency deviations within predefined safety limits and reduces the total operating cost of the distribution system [26]. Pang, K. et al. investigated the formation and scheduling methods of microgrids after disruptions, modeled the stochastic nature of load demand and distributed generation as joint chance constraints, and used them to construct a microgrid scheduling model, which can effectively guarantee the security of the scheduling process [27]. Yan, K. et al. showed that large-scale distributed energy access to the power grid will cause low inertia of the power system and reduce its frequency regulation ability, so the frequency characteristics and frequency response mode of the power system are analyzed from the point of view of "source-network-load-storage", and a method of operation optimization under the constraints of frequency security is proposed [28]. Guo, T. et al. proposed a source-load-storage game model with minimized operating cost and highest power quality of the microgrid system, aiming at balancing the interests of the power source, the load, and the energy storage aspects to ensure the safe and stable operation of the microgrid system [29]. Wang, C. et al. integrated distributed source-load into a DC microgrid virtual energy storage system based on the conversion relationship between distributed generation and capacitive energy storage, and thus established a source-load-storage cooperative optimization control strategy, which effectively alleviated the regulation pressure of DC microgrid energy storage [30]. He, X. et al. designed a microgrid smart generation control command assignment model based on a deep reinforcement learning framework, which takes into account the uncertainty of distributed source loads to achieve a safe and effective dynamic frequency regulation method [31]. Based on the flexible regulation potential and application scenarios of microgrids, the above analysis constructs an optimal scheduling model under distributed source-load uncertainty characterization and embeds the security of frequency regulation into the model in order to guarantee the stable operation of distribution networks under distributed source-load aggregation.

This paper establishes the uncertainty probability density function about the actual output of “source” and “load” side, constructs the mathematical model of distributed power supply and energy storage device of distribution network respectively, and carries out the research on the planning and allocation of distribution network capacity. Evaluation indexes such as DG investment and operation cost and network loss cost are used as objective functions to complete the construction of the comprehensive cost model for the optimization problem of distributed power capacity allocation. The power supply security of the distribution network is taken as the main constraint, and other operational constraints are combined to formulate the distributed power capacity optimization model. On the basis of the traditional sparrow search algorithm, the adaptive vigilance system is introduced so that it decreases nonlinearly with the increase of iteration number. The effectiveness of the adaptive sparrow search algorithm is verified through simulation experiments. Compare the source-load cooperative system and the effect of joint optimization and allocation of source-load cooperative and energy storage system, and analyze the operation effect of its cooperative strategy.

2. Distributed synergy of electric loads in distribution networks based on source-load uncertainty

2.1. *Source-load uncertainty analysis*

In order to ensure the accuracy and effectiveness of the proposed distributed cooperative control scheme for distribution network loads, the “source-load” uncertainty is considered. The probability distribution function is used to analyze the uncertainty of “source” and “load”.

2.1.1. Source-side uncertainty. The existence of uncertainty will inevitably lead to the existence of a certain error between the actual output of each “source” and the expected output. Based on this error, the probability density function of the uncertainty of the actual output of the “source” side is established, and the function expression is as follows:

$$p(a_i) = \frac{1}{\sqrt{2\pi} A_i} e^{-\frac{\Delta a_i^2}{2A_i^2}} \tag{1}$$

where: $p(a_i)$ is the uncertainty probability density function of the distributed power supply i on the “source” side, a_i is the actual output of the distributed power supply i, Δa_i is the error between the actual and expected output of the distributed power supply i, and A_i is the variance of the prediction error of the output of the distributed power supply i.

2.1.2. Uncertainty on the “load” side. Compared with the uncertainty on the “source” side, the uncertainty on the “load” side is much stronger, and many changes in external objective factors may trigger sudden changes in electricity load. The probability density function of the uncertainty of the actual output on the “load” side is established in [32]:

$$\zeta(c)=\frac{1}{\sqrt{2\pi Bc}}e^{-\frac{c(1-b)}{2B^2c}} \tag{2}$$

where: $\zeta(c)$ is the probability density function of the uncertainty of the actual output on the “load” side, c is the average value of the load, B is the standard deviation of the load, and b is the expected total load.

2.2. Distributed power capacity optimization allocation model

2.2.1. Distribution Network System Composition and Power Modeling. To plan and configure the capacity of the distribution network, it is first necessary to establish mathematical models for the main distributed power sources and energy storage devices contained within the distribution network, respectively. Fig. 1 shows the system structure, which demonstrates the main framework of a typical distribution network and the composition of distributed power sources within the distribution network. The distributed power sources involved are mainly wind generators (WG), photovoltaic generators (PV), diesel generators (DIE), and batteries (BS).

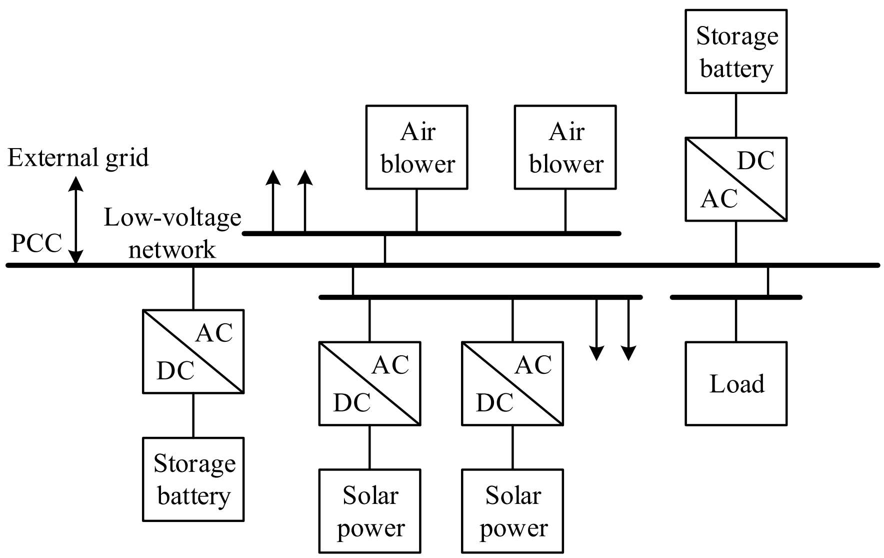

Fig. 1. System structure diagram

2.2.2. Wind turbines. Wind energy is a kind of clean renewable energy, but the wind speed is not controlled, and directly affects the output power of the fan, wind turbine output power P_{vt} and the wind speed v of the approximate relationship can be expressed in equation (3):

$$P_{w_g}(t)=\begin{cases}0, & v(t)<v_{in}\\ k_i v(t)^3-k_2P_n, & v_{in}<v(t)<v,\\ P_n, & v_r<v(t)<v_{out}\\ 0, & v(t)>v_{out}\end{cases} \tag{3}$$

where $k_1=P_nI(v_r^3-v_{in}^3), k_2=v_{in}^3I(v_r^3-v_m^3)$, P_n are the fan blade ratings, v_{in} is the cut-in wind speed, v_r is the rated wind speed, and v_{out} is the cut-out wind speed.

2.2.3. Photovoltaic generators. Photovoltaic energy is a renewable and clean energy source, as is wind energy, and the two have a complementary relationship in time. The output power P_{pm} of PV is related to the intensity of sunlight and ambient temperature, and the mathematical model of PV power output is shown in equation (4):

$$P_{pv}(t) = P_{stc}\frac{G_{ac}}{G_{stc}}[1 + k_3(T_c - T_r)] \tag{4}$$

where P_{sk} is the maximum output power of the solar cell under standard test conditions (25.0°C, 1.0 MPa), G_{ac} is the light intensity ($\mathrm{kW/m^2}$). G_{ste} is the light intensity under standard test conditions, taken as $1\,\mathrm{kW/m^2}$, k_3 is the temperature coefficient, taken as -0.4%/°C. T_c is the solar panel surface temperature in degrees Celsius, and T_r is the test reference temperature, taken as 25°C.

2.2.4. Diesel generators. The diesel electric generator (DIE) is a small controllable power source made of diesel fuel, and its power P_{die} is free to change as needed within the adjustable range, which belongs to the independent variable. Therefore, when establishing the diesel generator model, the cost of its fuel consumption as a dependent variable, the relationship between the cost of fuel consumption of diesel generator sets and the output power is shown in equation (5):

$$C_F(t) = aP_{die}^2(t) + bP_{die}(t) + c \tag{5}$$

where $C_r(t)$ and $P_{dir}(t)$ are the fuel cost and generation capacity of the diesel generator for t hours. a,b,c are the fuel curve coefficients, generally provided by the manufacturer, a,b,c which are 0.0071, 0.2333, and 0.4333, respectively.

2.2.5. Modeling of energy storage devices. Energy storage devices can effectively improve the uncontrollability of new energy generation and reduce the impact of the timing characteristics of renewable distributed power sources on system stability. Battery energy storage system (BESS) is mainly composed of four parts: battery system (BS), power conversion system (PCS), battery management system (BMS), and monitoring system, etc. The structure of BESS system is shown in Fig. 2.

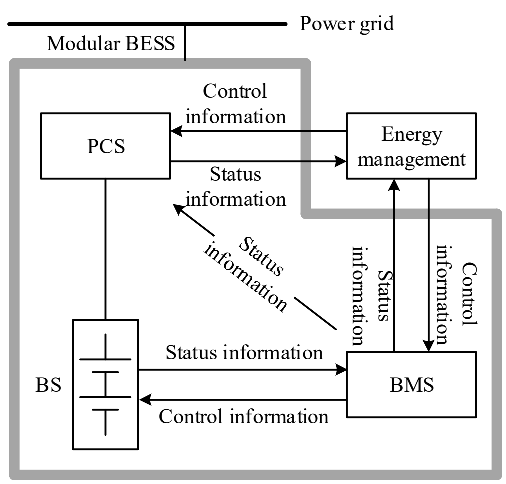

Fig. 2. Application of energy storage battery in power generator side

The above mentioned batteries have two states, charging and discharging, and the state of charge (SOC) is determined by a combination of the remaining power at the previous moment, the wind and solar power output, and the system load power [33]:

$$\begin{cases} P_{bat,out}(t) = P_{load}(t) - P_{re}(t) \\ S_{soc}(t+1) = S_{soc}(t) - \Delta t P_{bat,out}\, l\eta_a \end{cases} \tag{6}$$

$$\begin{cases} P_{bat,in}(t) = P_{re}(t) - P_{load}(t) \\ S_{soc}(t+1) = S_{soc}(t) + \Delta t P_{bat,in} / \eta_b \end{cases} \quad (7)$$

Equations (6) and (7) are the processes of battery output power and absorbed power, respectively. Where $P_{but,out}$ and $P_{but,in}$ are the battery discharge power and charging power, respectively, P_{re} is the sum of the output power of PV and WG, $P_{lout}(t)$ is the system load value at the moment of t, $s_{soc}(t)$ is the remaining battery power at the moment of t, Δt is the time interval between two adjacent calculations of the energy storage battery's charging state, which is taken as 1 hour in this paper, and η_a and η_b are the battery's discharging and charging efficiencies, respectively.

2.3. Distributed Power Capacity Optimization Model

2.3.1. Objective function. Considering that the node voltage fluctuation and network loss are important indicators for evaluating the power quality and economic advantages and disadvantages, respectively, the voltage stability margin and network loss are used as planning indicators, which are grouped together with the investment cost into a dimensionless comprehensive cost as the objective function. The comprehensive cost model for the capacity allocation optimization problem of distributed power supply is shown in equation (8):

$$F_{\min} = \omega_1 C_{invest} + \omega_2 C_{loxs} + \omega_3 C_u \quad (8)$$

where C_{invest} is the investment and operating cost of the distributed power source, C_{loss} is the cost of network losses in the system circuits, C_u is the cost of the voltage level penalties. $\omega_1, \omega_2, \omega_3$ is the weighting factor, and $\omega_1 + \omega_2 + \omega_3 = 1$, all costs covered in this chapter are annual costs.

1) Investment and operating costs of DG. The investment operating cost of DG consists of two parts: the discounted value of the construction investment cost of DG and the annual operating cost:

$$C_{invest} = C_{dg}\gamma + C_{run} \quad (9)$$

$$C_{dg} = S_{pv}C_{pv} + S_{wg}C_{wg} \quad (10)$$

$$C_{run} = S_{pv}C_{rpv} + S_{wg}C_{nvg}\gamma \quad (11)$$

$$\gamma = \frac{r(r+1)^{\lambda}}{\left[(r+1)^{\lambda} - 1\right]} \quad (12)$$

where c_{dv} is the construction cost of distributed power supply, S_m and S_{wg} are the number of PV generators and wind generators per unit capacity, and C_{pv} and C_{wg} are the required cost of construction per unit capacity of PV and WG, respectively. γ is the conversion factor, r denotes the discount rate, which is taken as 0.1, and λ is the service life of the system network. C_{run} is the unit operating cost of DG, c_{rpv} and C_{nwg} are the operating cost per unit capacity of PV and WG respectively.

2) Network loss cost

$$C_{loss} = c_f \sum_{i=1}^{N_L} \left(\frac{P_i^2 + Q_i^2}{U_i^2} r_i\right) \quad (13)$$

where c_f is the system electricity unit price, N_L is the number of system branches, P_i, Q_i is the active power and reactive power at the end node of the ith branch respectively, U_i is the voltage at the end node of the ith branch, and r_i is the resistance value of the ith branch.

3) Voltage offset rate. Considering that the node voltage is one of the important indexes characterizing the system stability and power quality, the node voltage will be increased after the DG is connected to the distribution network, but it is limited to the user's expectation, so the voltage offset rate index is:

$$C_u = \sum_{i=1}^{N_{iod}} \left(\frac{U_i - U_e}{U_p} \right)^2 \tag{14}$$

where, C_u is the voltage offset index, here the simulated voltage cost is carried out, N_{lowd} is the number of nodes with loads in the system, U_i is the voltage magnitude at the load nodes, U_e is the required voltage, and U_p is the permissible voltage deviation at the system nodes.

2.3.2. Constraints:

1) Investment constraints:

(1) Energy storage power and capacity constraints:

$$\begin{cases} \sum\limits_{i \in \Omega^{ess}} E_i^{ess} \le E_{total}^{ess} \\ 0 \le E_i^{ess} \le E_{i,\max}^{ess} \\ 0 \le P_i^{ess} \le P_{i,\max}^{ess} \\ P_{i,\max}^{ess} \rho = E_{i,\max}^{ess} \end{cases} \tag{15}$$

(2) DR capacity constraints:

$$\begin{cases} \sum\limits_{i \in \Omega^{dr}} P_i^{dr} \le P_{total}^{dr} \\ P_i^{dr} = 10\% x_i^{dr} P_{i,\max}^{load} \end{cases} \tag{16}$$

where: $E_{total}^{ess}, P_{total}^{dr}$ is the upper limit of the total allowable configuration of energy storage and DR, respectively, $P_{i,\max}^{ess}, E_{i,\max}^{ess}$ is the maximum value of the energy storage rated power and capacity at node i, respectively, ρ is the power-to-capacity ratio of the energy storage device, x_i^{dr} is the integer decision variable of DR at node i, which in this paper takes the value range of [0, 5], and is multiplied with the percentage coefficient to express the relationship between the maximum load of the node and the capacity of the allocated DR, and $P_{i,\max}^{load}$ is the maximum load at node i [34].

2) Operational constraints:

(1) Equation constraints of AC branch circuit tidal equations:

$$\begin{cases} \sum\limits_{k(i,:) \in \Omega^L} P_{k,s,t} - \sum\limits_{k(:,i) \in \Omega^L} (P_{k,s,t} - I_{k,s,t}^2 R_k) = P_{i,s,t}^{inj} \\ \sum\limits_{k(i,:) \in \Omega^L} Q_{k,s,t} - \sum\limits_{k(:,i) \in \Omega^L} (Q_{k,s,t} - I_{k,s,t}^2 X_k) = Q_{i,s,t}^{inj} \end{cases} \tag{17}$$

$$\begin{cases} P_{i,s,t}^{inj} = P_{i,s,t}^{D} + P_{i,s,t}^{pvg} + P_{i,s,t}^{dec} + P_{i,s,t}^{dis} - P_{i,s,t}^{ch} - P_{i,s,t}^{inc} - P_{i,s,t}^{load} \\ Q_{i,s,t}^{inj} = Q_{i,s,t}^{D} + Q_{i,s,t}^{pvg} + Q_{i,s,t}^{dec} - Q_{i,s,t}^{inc} - Q_{i,s,t}^{load} \end{cases} \tag{18}$$

$$U_{j,s,t}^2 = U_{i,s,t}^2 - 2(P_{k,s,t}R_k + Q_{k,s,t}X_k) + I_{k,s,t}^2(R_k^2 + X_k^2)\forall k(i,j) \in \Omega^L \tag{19}$$

$$I_{k,s,t}^2 U_{i,s,t}^2 = P_{k,s,t}^2 + Q_{k,s,t}^2 \forall k(i,j) \in \Omega^L \tag{20}$$

where: Ω^L is the set of distribution network branches, i, j is the node number, $k(i,:)$ represents the branch with i as the first end, $k; k(:,i)$ represents the branch with i as the end, k, $P_{k,s,t}, Q_{k,s,t}, I_{k,s,t}$ is the active and reactive power and current on branch k, respectively. R_k, X_k is the value of resistance and reactance on branch k, $U_{i,s,t}$ is the node voltage, $P_{i,s,t}^{inj}, Q_{i,s,t}^{inj}$ indicates the active and reactive power injected at node i. $P_{i,s,t}^{pvg}, P_{i,s,t}^{load}, P_{i,s,t}^{inc}$ are the actual PV active output, distribution network active load, and active power added by DR transfer, and $Q_{i,s,t}^{pvg}, Q_{i,s,t}^{load}, Q_{i,s,t}^{inc}, Q_{i,s,t}^{dec}$ are the PV reactive output, distribution network reactive load, reactive power added by DR transfer, and reduced reactive power, respectively.

(2) Distribution network security constraints:

$$0 \le I_{k,s,t} \le I_{k,\max} \tag{21}$$

$$U_{i,\min} \le U_{i,s,t} \le U_{i,\max} \tag{22}$$

where: $I_{k,\max}$ is the maximum current limit of branch k.

(3) Light abandonment constraint:

$$P_{i,s,t}^{PVG} = P_{i,s,t}^{pvg} + \Delta P_{i,s,t}^{pvg} \tag{23}$$

$$0 \le P_{i,s,t}^{pvg} \le P_{i,s,t}^{PVG} \tag{24}$$

where: $P_{i,s,i}$ is the predicted power generation of distributed PV i at the s scenario t moment, and Eq. (23) represents the sum of PV power $\Delta P_{i,s,t}^{pvg}$ abandonment and actual utilization $P_{i,s,t}^{pvg}$ is equal to the predicted power generation.

(4) Energy storage dynamic operation constraints:

$$(S_{soc,i,t+1} - S_{soc,i,t})E_i^{ess} = (P_{i,s,t}^{ch}\eta^c - P_{i,s,t}^{dis}/\eta^d)\Delta t \tag{25}$$

$$S_{soc,i,0} = S_{soc,i,T} \tag{26}$$

$$0 \le P_{i,s,t}^{ch}\eta^c \le P_i^{ess} Z_{i,s,t}^{ess} \tag{27}$$

$$0 \le P_{i,s,t}^{dis}/\eta^d \le P_i^{ess}(1 - Z_{i,s,t}^{ess}) \tag{28}$$

Eq. (25) is the charge state constraint, $S_{soc,i,i}$ is the charge state of the energy storage at the moment of t, and $P_{i,s,t}^{ch}, P_{i,s,t}^{dis}$ is the charge/discharge power of the energy storage, respectively. Eq. (26) is the charging and discharging conservation constraint, which ensures that the energy storage has the same charging and discharging capacity in the next scheduling cycle. Eqs. (27) and (28) are the charging and discharging power constraints, η^c, η^d is the charging and discharging efficiency, respectively, and $Z_{i,s,t}$ is the charging and discharging state 0-1 variable.

(5) DR dynamic operation constraints:

$$\sum_{t=1}^{T} P_{i,s,t}^{inc} - \lambda_i \sum_{t=1}^{T} P_{i,s,t}^{dec} = 0 \tag{29}$$

$$0 \le P_{i,s,t}^{dec} \le \min\{P_i^{dr}, P_{i,s,t}^{load}\} \tag{30}$$

where: λ_i is the load transfer ratio, which is formulated according to different load types and user demands. Although the load response characteristics of different incentive type DRs differ, Eq. (29) can all describe the relationship between transferred power and curtailed power to characterize the power balance during the operating hours.

3. Distributed power capacity allocation model solving

3.1. Sparrow Search Algorithm

3.1.1. Traditional Sparrow Search Algorithm:

1) Initialization. Starting from the initial N sparrows, the virtual sparrows are used to find food and the locations of the sparrows can be represented by the following matrix:

$$X = \begin{bmatrix} X_{11} & X_{12} & \cdots & \cdots & X_{1d} \\ X_{21} & X_{22} & \cdots & \cdots & X_{2d} \\ \vdots & \vdots & \vdots & \vdots & \vdots \\ X_{N,1} & X_{N,2} & \cdots & \cdots & X_{N,d} \end{bmatrix} \tag{31}$$

where, N is the number of sparrows, d is the dimension of the variable to be optimized, and X_{Nd} is the d th dimension value of the N th sparrow. The fitness values of all the sparrows can be represented by the following vector:

$$F_X = \begin{bmatrix} f([X_{1,1} & X_{1,2} & \cdots & \cdots & X_{1,d}]) \\ f([X_{2,1} & X_{2,2} & \cdots & \cdots & X_{2,d}]) \\ \vdots & \vdots & \vdots & \vdots & \vdots \\ f([X_{N,1} & X_{N,2} & \cdots & \cdots & X_{N,d}]) \end{bmatrix} \tag{32}$$

The value of each row in F_X represents the adaptation value of an individual, and the adaptation value is used as an evaluation index to rank N sparrows according to the quality of the food found, and the top 20% of the sparrows are selected as the discoverers, and the rest of the sparrows are the followers.

2) Discoverer position update. When $R_2 < ST$, it means that there is no predator around the foraging environment at this time, and the finder can perform extensive search operation, if $R_2 > ST$, it means that some sparrows in the population have found the predator and alerted the other sparrows in the population, at this time, all the sparrows need to quickly fly to other safe places for foraging:

$$X_{i,t}^{L+1} = \begin{cases} X'_{i,t} \cdot \exp\left(\dfrac{-i}{\alpha \cdot iter_{\max}}\right) & \text{if} \quad R_2 < ST \\ X'_{i,t} \cdot Q \cdot L & \text{if} \quad R_2 \ge ST \end{cases} \tag{33}$$

where t represents the current iteration number, $j = 1,2,3,\cdots,d$, $X'_{i,t}$ represent the j th dimensional values of the ith sparrow of the tth generation. Q is a random number obeying normal distribution, $\alpha \in (0,1]$ is a random number, $iter_{\max}$ is the maximum number of iterations, and L is an d -dimensional row vector, where each element is 1. $R_2 (R_2 \in [0,1])$ and $ST (ST \in [0.5,1])$ denote the warning value and safety threshold, respectively.

3) Follower position update. The follower position update mechanism is shown in equation (34):

$$X_{i,j}^{i+1}=\begin{cases} Q\cdot\exp(\dfrac{X_{worg}^{t}-X_{i,j}^{t}}{i^2}) & \text{if } i>N/2 \\ X_{p}^{t+1}+|X_{i,j}^{t}-X_{p}^{t+1}|\cdot A^{t}\cdot L & \text{else} \end{cases} \tag{34}$$

where Q is a random number obeying a normal distribution, x_r^{t+1} is the best position occupied by the current producer, X_{nom}^{t} is the worst position globally, L is a d-dimensional row vector where each element is 1, and A is a 1% matrix where each element is randomly assigned either 1 or -1, and there is a $A^{+}=A^{T}(AA^{T})^{-1}$. At $i>N/2$, this indicates that the ith follower with the lower fitness value did not get food and is in a very hungry state, and at this point needs to fly in other places to perceive food to get more energy.

4) Detection and early warning mechanism. Randomly selected SD individuals in each generation of the population have the behavior of detecting dangers and alerting the population to help the population stay away from dangerous areas, which is conducive to improving the evolutionary level of the population as a whole. The formula for updating the position of the vigilant is as follows:

$$X_{i,j}^{t+1}=\begin{cases} X_{ben}^{t}+\beta\cdot|X_{i,j}^{t}-X_{ben}^{t}| & \text{if } f_i>f_g \\ X_{i,j}^{t}+K\cdot\left(\dfrac{|X_{i,j}^{t}-X_{woni}^{t}|}{(f_i-f_w)+\varepsilon}\right) & \text{if } f_i=f_g \end{cases} \tag{35}$$

where X_{ket}^{t} is the optimal position of all individuals globally. β, as a step control parameter, is a random number that obeys a normal distribution with mean 0 and variance 1. $K\in[-1,1]$ is a random number, and f_i is the fitness value of the current sparrow individual. f_x and f_w are the current global best and worst fitness values, respectively. ε is the smallest constant to avoid zero in the denominator.

3.1.2. Adaptive Sparrow Search Algorithm:

1) Chaotic initialization. In this paper, the sequence of cubic mapping is utilized to help the sparrow search algorithm to obtain the initial individual that traverses the whole globe, and the chaotic cubic mapping formula is shown in (36):

$$y(n+1)=4y(n)^3-3y(n),-1\le y(n)\le 1,n=1,2\cdots \tag{36}$$

In order to obtain N d-dimensional vector shown in Eq. (31), which forms the sparrow population, there are three steps to generate a chaotic sequence using chaotic cubic mapping:

(1) The first sparrow in the d-dimensional space is randomly generated with the expression shown in (37):

$$Y=(y_1,y_2,y_3\cdots,y_d)\quad y_d\in[-1,1] \tag{37}$$

(2)Starting from the natural sparrow shown in Eq. (37), iterate each dimension of each sparrow N-1 times according to Eq. (36) one by one to obtain N-1 artificial sparrows.

(3) A total of N sparrows are obtained and mapped into the search space according to Eq. (38):

$$x_{i,d}=L_d+(1+y_{i,d})\times U_d-L_d{}^2 \tag{38}$$

where U_d and L_d are the upper and lower bounds of the search space, y_{id} is the d-dimensional coordinate of the ith artificial sparrow, and $x_{i,d}$ is the d-dimensional coordinate of the pseudo-random sparrow in the ith search space.

2) De-originization operation. From the producer position update formula (33) in SSA, it can be seen that when $R_2 > ST$, the finder moves randomly to the current position according to the normal distribution, i.e., converges to the current optimal position. When $R_2 < ST$, it is a step for the particle to jump out of this position. Because $\exp(-i/\alpha \cdot iter_{\max}) \le 1$, means that the value of each dimension of the particle decreases after each iterative update, in order to make the algorithm solve the model better, a de-originization operation is performed on the escape direction of the SSA producer as shown in Eq. (39):

$$x_{i,d}^{t+1} = \begin{cases} x_{i,d}^{t} \cdot (1+Q) & \text{if} \quad R_2 < ST \\ x_{i,d}^{t} + Q & \text{if} \quad R_2 \ge ST \end{cases} \tag{39}$$

Q denotes a random number obeying a normal distribution, and $x_{i,d}^{t}$ is the dth dimensional value of the ith individual in the trd generation population. That is, the direction in which the discoverer leaves the current position is no longer toward the origin, and the update strategy is to multiply with a normally distributed random number $1+Q$ with mean 1 and variance 1.

3) Adaptive alert coefficient. In this paper, we introduce an adaptive mechanism for the parameter ST so that it decreases nonlinearly with the increase in the number of iterations.The formula for the change of ST is shown in Equation (40):

$$ST = 0.9 - \frac{\exp\left[\dfrac{10(t-1)}{iter_{\max}-1}\right]-1}{2(e^{10}-1)} \tag{40}$$

where ST is the safety threshold, t is the current number of iterations, and $iter_{\max}$ is the maximum number of iterations.

3.2. Algorithm validation

3.2.1. Multi-objective optimization results. In this paper, in order to solve the problem of optimal allocation of distributed power capacity in distribution grid system, adaptive sparrow search algorithm (ASSA) is used to perform multi-objective optimization of the capacity of three commonly used distributed power sources, namely wind turbine, photovoltaic, and energy storage, the capacity of the three power sources is used as variables to construct the sparrow individual, the minimization cost function is used as the fitness function for the optimization search, and the required wind speed is calculated by using the models of wind turbine, photovoltaic, and energy storage, The wind speed, solar radiation intensity, temperature, and load power data required for the modeling of wind turbine, PV, and energy storage are used as inputs to obtain the optimal configuration of distributed power sources. Because the cost calculation needs to consider at least one year's cost to be more meaningful, so collect the hour-by-hour wind speed, solar radiation intensity, temperature and load power data around a substation in one year as inputs, Fig. 3 shows the hour-by-hour wind speed, temperature, solar radiation, and load power data of a distribution network, and Figs. (a)-(d) show the wind speed, temperature, solar radiation intensity and load power, respectively. The wind speed is 16.915m/s at 5050h, the temperature reaches the maximum value of 60.04°C at 4037h, the maximum value of solar radiation intensity is 1158.961w/m^2, and the load power is maintained within 500kW.

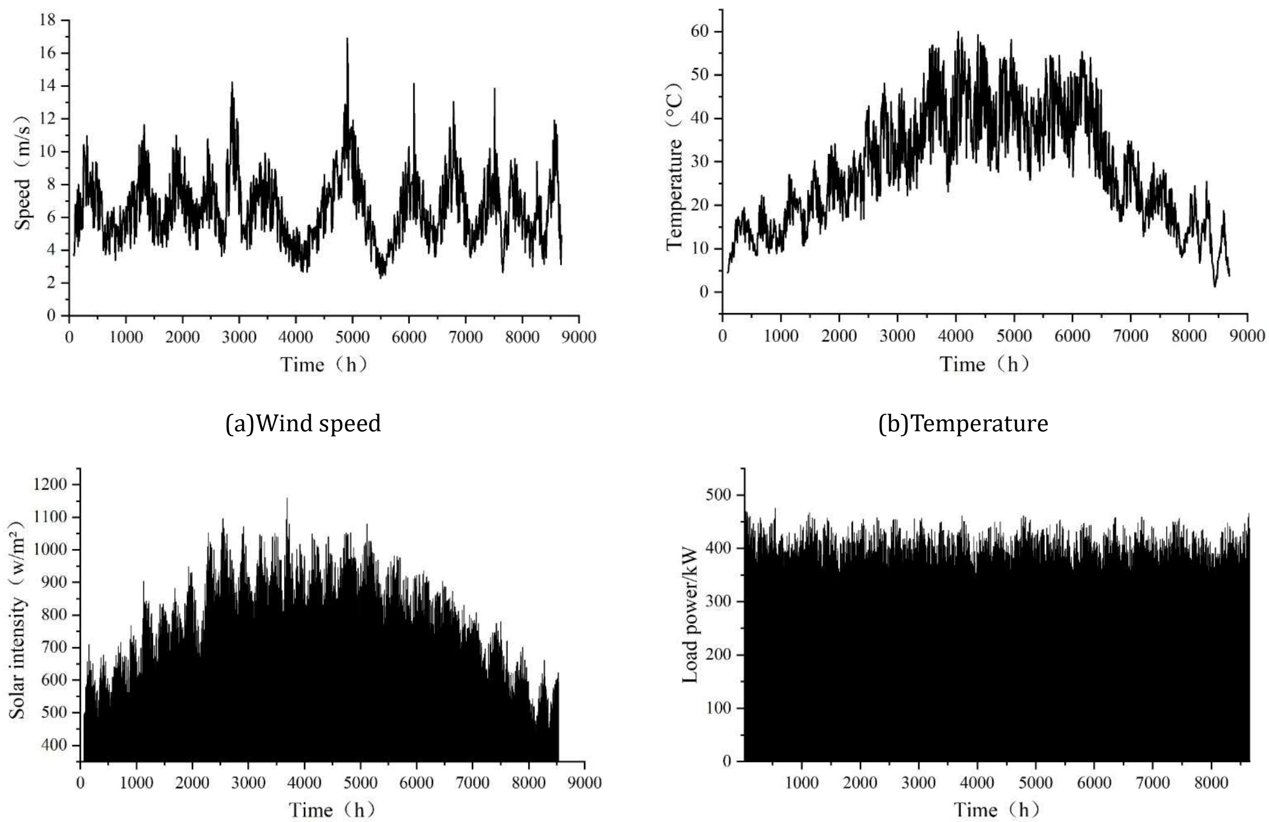

(a)Wind speed

(b)Temperature

(c)Solar radiation intensity

(d)Load power

Fig. 3. A distribution network data

3.2.2. Optimal Capacity Analysis. In the objective function calculation, the main parameters of the cost calculation are set as shown in Fig. 4, and the construction costs of the wind turbine model, the PV model, the diesel model, and the energy storage device are 810, 1500, 950, and 1100 yuan- kW^{-1}, respectively.In the wind turbine model, v_{ci} is 2.5 m/s, v_r is 12 m/s, and v_{co} is 18 m/s. In the PV model, the power temperature coefficient k is - 0.0038. In the cost function calculation, the capital discount rate r is 0.12. In the ASSA algorithm, the population size is set to 30, the conversion probability is 0.8, and the maximum number of iterations is 500. The upper limit of capacity is 10 times the maximum load power, and the total optimal capacity is required not to exceed this limit.

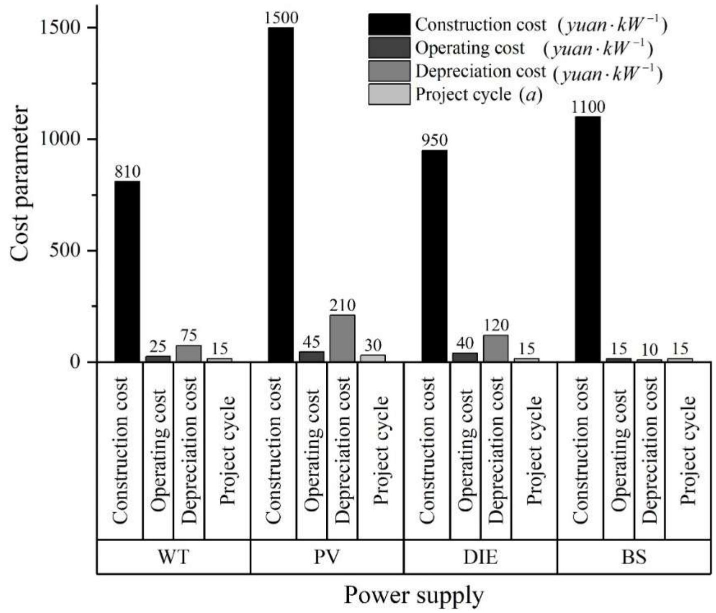

Fig. 4. Parameters related to costing

In this paper, the adaptive sparrow search algorithm is used to optimize the capacity of common distributed power sources in the distribution network under the new power system environment, and the results of the optimal capacity and the corresponding benefits are shown in Fig. 5. In the optimal capacity composition, the optimal capacity of photovoltaic accounts for the largest proportion of the overall optimal capacity, with a capacity of 1250 kW, and the wind turbine accounts for the smallest proportion of the overall capacity. In the cost composition, the largest share is for PV (2,846,400 yuan), and the smallest share is for wind turbine (914,800 yuan), which is due to the fact that PV has the highest unit price for construction investment and O&M, which raises the cost incurred. Therefore, in the process of distribution network distributed power allocation, under the premise of meeting the conditions, we can consider increasing the capacity allocation of wind turbines and reducing the capacity allocation of photovoltaic, so as to reduce the cost brought about.

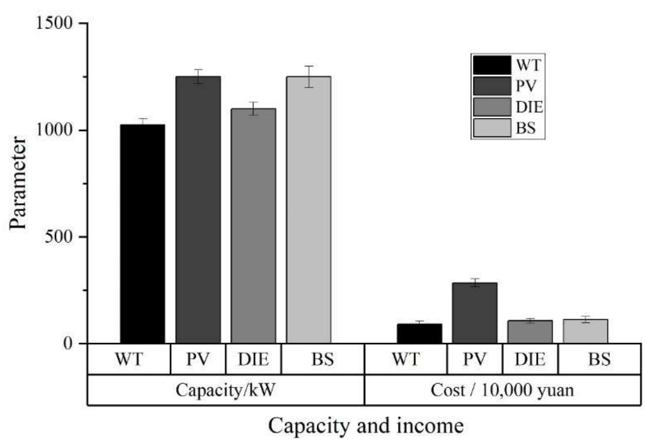

Fig. 5. The best capacity and the corresponding benefits

3.2.3. Adaptive Sparrow Search Algorithm Analysis. In order to prove the effectiveness of the adaptive sparrow search algorithm proposed in this paper, the adaptive sparrow search algorithm and the unimproved sparrow search algorithm are used to simulate respectively, the parameters of the unimproved sparrow search algorithm are set to the number of populations of 30, the conversion probability of 0.8, and the maximum number of iterations is 500, and the results are shown in Figure

6. The improved adaptive sparrow search algorithm converges faster and there is no local convergence, no large deviation after convergence, and the cost function is less than 5×10^{6} when the number of iterations exceeds 339. It is proved that the adaptive sparrow search algorithm is effective and the adaptive sparrow search algorithm has significant improvement.

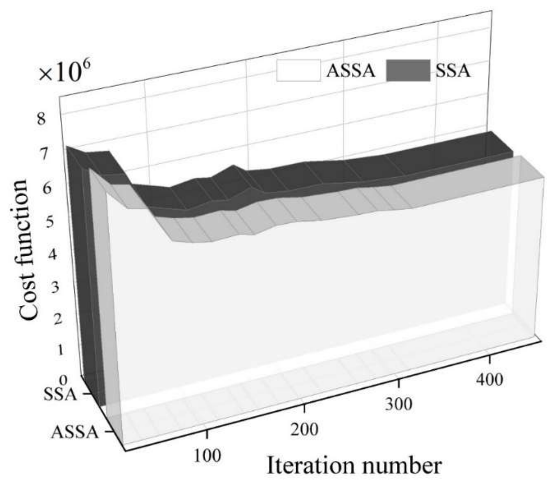

Fig. 6. ASSA is compared to SSA

4. Distributed source-load aggregation and capacity optimization considering security of supply in distribution networks

4.1. *Analysis of Distributed Source-Load Aggregation Optimization Configuration Strategy*

4.1.1. Distributed source-load cooperative planning. In this paper, we study that the distribution grid can promote distributed photovoltaic (DPV) power consumption through the cooperative scheduling of flexibility resources, and to this end, we propose a joint optimal allocation method of DPV and energy storage system (ESS) with source-load synergy.

This section focuses on the joint planning of DPV and ESS with source-load synergy and the economic analysis of distribution network after considering energy storage. Table 1 shows the results of the co-optimized allocation and the cost comparison. It should be noted that the DPV and ESS joint planning analysis sets the upper limit of the integrated cost of the distribution network to the annual integrated cost of DPV planning alone.

Compared to the DPV plan, the joint DPV and ESS plan enhances the installed capacity of DPVs by about 13.45%. The total generation capacity of DPVs in the distribution system increases by about 13.09%. From the abandoned light cost, it is clear that the abandoned light of the joint planning is higher relative to the DPV alone planning, which is caused by the DPV installation capacity enhancement. Calculating the average power generation per unit capacity of DPV, the average power generation of the joint planning scheme is 88.35 kW/h, while that of the DPV alone planning is 88.4 kW/h. It is obvious that the joint planning significantly enhances the installed capacity of DPV under the condition of slightly increasing the DPV curtailment.

The cost of the Joint Planning Program is significantly lower than the cost of DPV planning alone, a reduction of approximately 26.06%. Although the joint planning increases the ESS construction/operation and maintenance cost (1,582,365,000 RMB), and the cost of light abandonment and flexible load compensation cost is slightly higher compared to the DPV individual planning scheme, the joint planning significantly reduces the main grid power purchase cost through the enhancement of DPV power consumption, and improves the economics of the distribution network.

In addition, ESS to-be-selected location changes can affect the DPV and ESS planning results, and certain to-be-selected nodes do not even need to install ESS. The energy storage configuration node should generally be close to the DPV access point. It should be noted that the actual planning can be determined on a case-by-case basis after the ESS to-be-selected location is determined for the planning study.

Table 1. Collaborative optimization of configuration results and cost comparison

Node	DPV Access capacity/MW	
	DPV/ESS collaborative planning	DPV planning
32	2.8411	2.6315
34	3.8762	3.3952
43	5	3.4132
47	2.1956	2.8236
Sum total	**13.9129**	12.2635
Install node	Installation apparent power /kW	Installed capacity/(kW· h)
23	650	850
30	380	560
42	430	720
48	420	530
Argument	Numerical value	
	DPV planning	DPV/ESS collaborative planning
Total power generation/(MW· h)	9463.4235	10702.6545
Comprehensive cost of distribution network/10000 yuan	1387.9974	1026.2915
Storage and construction/operation and maintenance costs/10000 yuan	-	158.2365
Response load cost/10000 yuan	95.3185	128.3546
Cost of light abandonment/10000 yuan	15.7365	19.0568
Cost of purchasing electricity/10,000 yuan	1276.9424	720.6436

4.1.2. Source-load synergy analysis. In order to study the impact of source-load synergy on DPV consumption in distribution networks, this paper sets up eight scenarios to be analyzed, and Fig. 7 shows the results of DPV allocation under each flexible resource allocation scenario, and Fig. 8 shows the integrated cost of the distribution network and the total DPV generation capacity.

Comparing Scenario 1 to Scenario 8, the sum of DPV planning capacity increases gradually, and Scenario 8 has the best planning result, which is 42.89% higher than Scenario 1. When DPV access capacity planning is performed by considering one of the categories of grid-side (security of supply), source-side (DPV curtailment), and load-side (ESS with responsive loads) (corresponding to Scenarios 2, 3, and 4), the DPV capacity results are increased by 12.59%, 15.66%, and 16.68%, respectively, compared to Scenario 1, in which the ESS access to the distribution network can increase the DPV access capacity of the distribution network in a more substantial way. Scenarios 5, 6, and 7, whose DPV access capacity results are improved by 25.18%, 28.56%, and 36.23%, respectively, compared with Scenario 1, show that DPV curtailment, responsive load, and ESS synergistic planning can dynamically adjust the source-load output curves, thus promoting DPV consumption in the distribution network.

The total generation of DPVs in Scenarios 1 to 8 gradually increases, while the total cost of the distribution network fluctuates and changes. In Scenarios 2, 3, and 5, the consideration of power supply security constraints and DPV curtailment means leads to an increase in the integrated cost of the distribution network, which is analyzed because the distribution security constraints can adjust the system voltage and change the tidal current distribution so that the DPVs are better consumed, but their network losses also increase.

In addition, comparing Scenario 8 with the DPV joint planning results in Section 4.1.1, the DPV optimized capacities of the two scenarios are 13.96 MW and 13.91 MW, respectively, but the total generation capacity of the two scenarios are 10005 MW·h and 10702.6545 MW·h, respectively, and the integrated cost of the distribution network is 17.56 million and 10,262,915 MW. Since Scheme 8 does not consider the cost constraints of distribution network power supply security, its energy storage configuration capacity is much larger than the DPV joint planning scheme, and the planning capacity of DPV is not improved, the above results show that continuing to increase the storage capacity configuration at this time will not improve the planning capacity of DPV, and the economy of the system will also be reduced.

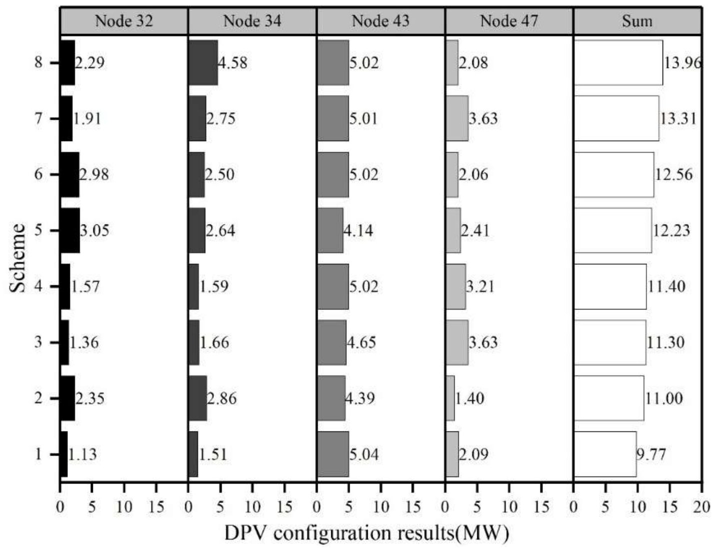

Fig. 7. The DPV configuration results in flexible resource allocation schemes

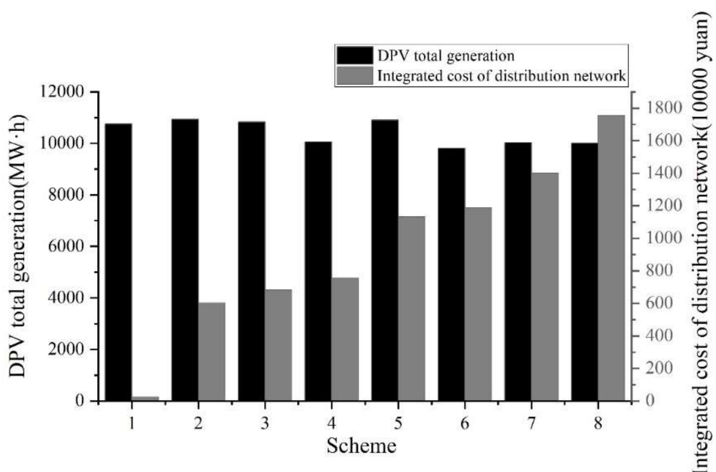

Fig. 8. Combined cost of distribution network and total power generation of DPV

4.1.3. Sensitivity analysis of reduction rates. In order to study the impact of DPV cut rate on DPV consumption and ESS joint planning, the maximum cut rate of PV is set to vary from 1% to 10% for DPV cut rate sensitivity analysis.The trend of total ESS installed capacity is shown in Fig. 9, and the distribution network cost comparison is shown in Fig. 10.

With the change of DPV reduction, the total installed capacity of ESS shows a decreasing and then increasing trend. When DPV reduction is small, the planned capacity of DPV in the distribution network is relatively small, and in order to ensure the efficient consumption of DPV, the installed capacity of ESS is larger. With the increase of DPV reduction, DPV can be efficiently consumed after reduction, so the installed capacity of ESS decreases. When the DPV reduction reaches 5%, the ESS installation capacity is the smallest, and the apparent and actual capacities are 1.3485 MV·A and

1.7045 MW·h, respectively. When the DPV reduction rate continues to increase, the DPV reduction does not effectively dissipate the DPV power due to the DPV access capacity of the distribution network becoming larger, and the ESS installed capacity shows a rising trend again, i.e., ESS needs to be increased to promote DPV consumption.

The comprehensive cost of the distribution network shows a decreasing and then increasing trend with the DPV reduction rate, and reaches the minimum value when the reduction rate is 5%, at which time the distribution network has the highest operating economy and the comprehensive cost of the distribution network is 9.83 million yuan. When the DPV reduction is 1% to 5%, the comprehensive cost of the distribution network shows a decreasing trend due to the reduction of ESS installation capacity and the increase of DPV access capacity, and the DPV reduction is greater than 5%. After the DPV reduction is greater than 5%, the comprehensive cost shows an upward trend due to the increase of DPV access capacity, reduction cost, and ESS installation cost.

In summary, if the focus of distribution network operation is economy, it is more appropriate to choose 5% for the maximum DPV reduction rate, and if it is more appropriate to choose 10% to improve the DPV consumption capacity of distribution network, this scheme can balance the economy of distribution network and DPV consumption capacity.

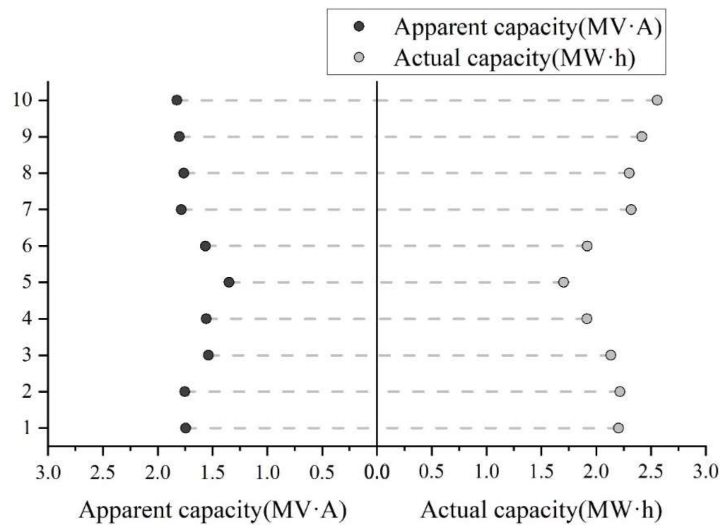

Fig. 9. The ESS assembly total capacity change trend

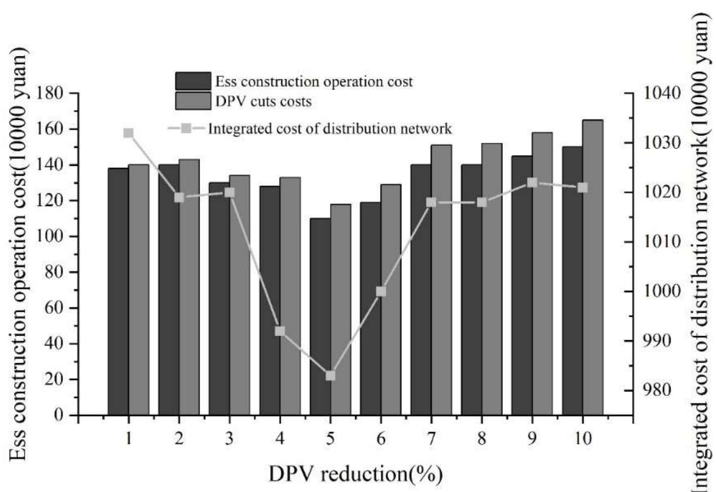

Fig. 10. Comparison of cost distribution

4.2. Analysis of Capacity Optimization Results

4.2.1. Hybrid power generation systems. In this paper, we will take Wai Lingding Island of ZH City as a project implementation site to optimize the power capacity of the hybrid power generation system, in order to verify the practical application of the proposed adaptive sparrow search algorithm in configuring the power capacity of the hybrid power generation system.

4.2.2. Algorithm Simulation and Result Analysis. In this paper, the arithmetic example is carried out in software Matlab 2021 to optimize the power capacity allocation of this hybrid power generation system using adaptive sparrow search algorithm. The system is dynamically simulated with a sampling time of 1 h, taking into account the environmental resource situation and electricity load of Wai Lingding Island.

Fig. 11 shows the cyclic charging scheme, Fig. (a) shows the annualized cost, and Fig. (b) shows the battery charge state. Fig. 12 shows the load following operation scheme, Fig. (a) shows the annual averaged cost, and Fig. (b) shows the battery charge state.

The cyclic charging operation scheme is used to maximize the output power of the diesel generator, thus effectively reducing the number of renewable energy generating equipment, and the annual averaged cost is smaller compared to the load-following operation scheme, with an initial operating cost of 536,698,000 yuan, and stabilized at 268,652,000 yuan after the number of iterations is 27 times.

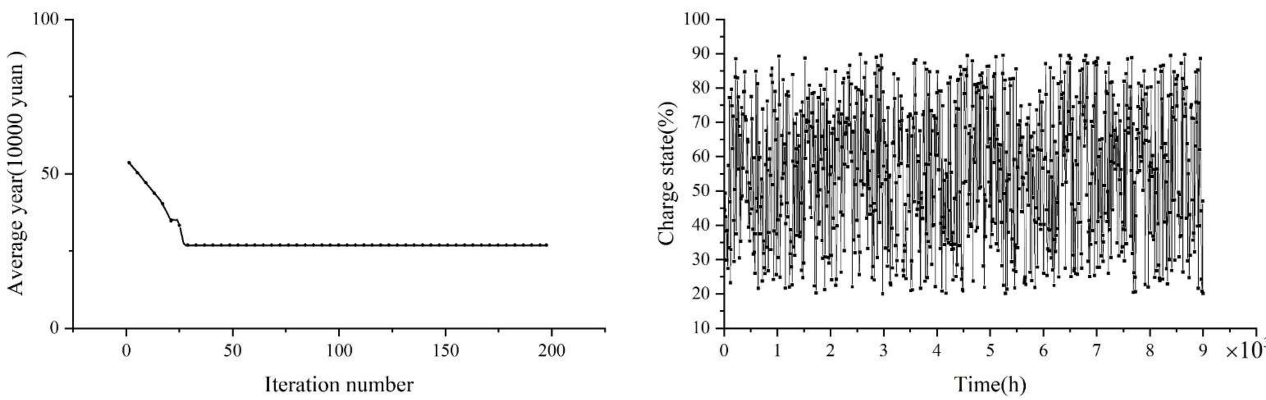

(a)Annualized costs (b)The battery is charged

Fig. 11. Cyclic charging scheme

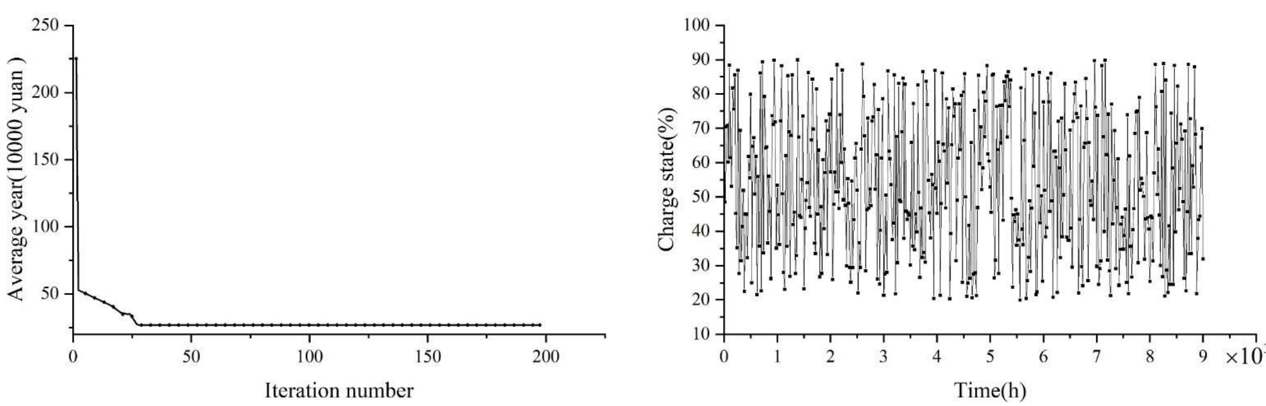

(a)Annualized costs (b)The battery is charged

Fig. 12. Load follows operation scheme

Of course, there are diesel generators due to longer working hours and lead to a substantial increase in pollution control and fuel costs, which is not conducive to the energy saving and emission reduction of the entire power generation system. The battery using cyclic charging operation scheme and load tracking operation scheme results for comparison, Table 2 for the optimization results of the two schemes, the use of cyclic charging operation scheme costs than the use of load tracking scheme costs lower 81,067 yuan, the economic effect has been significantly improved. The main difference between these 2 schemes lies in the utilization of the output power of the diesel generator.

Table 2. Optimization of the two schemes

Argument	Operation scheme	
	Cyclic charging	Load tracking
N_{WT} / number	2	3
N_{BS} / number	36	48
N_{PV} / number	250	400
Diesel working hours/h	512	313
Average year/yuan	276496	357563

5. Conclusions and outlook

5.1. Conclusion

In this paper, we consider the uncertainty on both sides of "source-load", and use the probability distribution function to explore the uncertainty on both sides of "source" and "load" respectively. We construct a distributed power capacity optimization model, take the security of power supply of distribution network as the constraint, set the relevant objective function and constraints, and use the adaptive sparrow search algorithm to solve the model.

1) Verify the effectiveness of the adaptive sparrow search algorithm, the improved adaptive sparrow search algorithm converges faster and there is no local convergence, there is no large deviation after convergence, and the cost function is less than 5×10^{6} when the number of iterations exceeds 339.

2) The capacity optimization configuration analysis of distributed source-load cooperative planning, the average power generation is 88.35kW/h under the cooperative optimal configuration of source-load cooperative DPV and energy storage system, while the DPV alone planning is 88.4kW/h, the joint planning obviously enhances the DPV installation capacity under the condition of slightly increasing the amount of DPV reduction.

3) The adaptive sparrow search algorithm is used to optimize the power capacity allocation of this hybrid generation system, and the model gives 2 scenarios, and comparing the optimization results of the 2 scenarios, the cost of using the cyclic charging operation scenario is 81,067 yuan lower than that of using the load tracking scenario, and the economic effect has been significantly improved.

5.2. Outlook

This paper takes the Wai Lingding Island of ZH City as the implementation point of the project, mainly from the perspective of the wind power storage power capacity allocation and actual operation of the Wai Lingding Island synergistic optimization of two-layer planning model construction, multi-objective solution set decision-making to carry out the research work on the optimization of the distributed source and load synergistic capacity allocation, and simulation to verify the effectiveness of the configured scheme in improving the power quality of the distribution network of the Wai Lingding Island of ZH City. Nevertheless, there are still many deficiencies and places that need further in-depth research, which are mainly categorized into the following aspects:

1) Although the ASSA algorithm performs well in the capacity applications of three commonly used distributed power sources, namely wind turbine, photovoltaic, and energy storage, it still needs to face different environments and conditions in practical applications. Different light intensities, different component types, and different climatic conditions will have an impact on the dynamic characteristics of the distributed source-load synergistic capacity system, thus affecting the performance of the ASSA algorithm. In order to further improve the performance of the ASSA algorithm, future research can use multiple variant strategies, explore more effective optimization search methods, as well as combine the ideas of other algorithms and practical environments to

design more flexible and efficient power capacity optimization control strategies. The ASSA algorithm has superior performance in simulation analysis, and future research work can be extended in the direction of practical application to further improve the applicability of the algorithm and the performance of the ASSA algorithm in practical distributed source-load cooperative systems.

2) In this paper, when carrying out the research work on the optimized allocation of distributed source-load cooperative capacity in Wai-lingding Island of ZH City, the focus is on the impact of the access of distributed power sources of wind power and storage on the network losses as well as the voltage level of the distribution network in Wai-lingding Island of ZH City, and in the future, more important power quality evaluation indexes, such as load fluctuation, voltage stability, and so forth, may be introduced in order to further enhance the comprehensiveness of the allocation scheme. Meanwhile, the follow-up work can focus on studying the cooperative working mechanism of different types of DG, such as micro-gas turbines, hydroelectric power plants, and so on.

3) Demand-side management (DSM), as an important means of regulating grid load and optimizing energy distribution, has unique value and potential in active distribution networks. Future research could explore how to better integrate DPV and ESS through highly flexible and responsive demand-side management measures to maximize the economic operation and environmental benefits of the grid.

4) Though the two-layer optimization model of DPV and ESS can describe the planning process more effectively than single-layer optimization, its computational process is too complicated, with a large amount of arithmetic, and the upper and lower iteration processes are easily confused. Therefore, the solution method of the model can be explored and the solution idea can be converted to reduce the computational complexity under the premise of ensuring the computational accuracy.

Funding

State Grid Fujian Economic Research Institute Special Project Funding (NO. B3130N24000M).

References

[1] Guo, X., Gan, L., Liu, Y., & Hu, W. (2023). Coordinated dispatching of flexible AC/DC distribution areas considering uncertainty of source and load. Electric Power Systems Research, 225, 109805.

[2] Zhang, H., Ji, X., Wang, W., Li, M., & Zhang, J. (2024, June). Study on enhanced new energy source-load interaction response strategy based on multiple time scales. In Journal of Physics: Conference Series (Vol. 2781, No. 1, p. 012020). IOP Publishing.

[3] Li, C., Feng, C., Li, J., Hu, D., & Zhu, X. (2023). Comprehensive frequency regulation control strategy of thermal power generating unit and ESS considering flexible load simultaneously participating in AGC. Journal of Energy Storage, 58, 106394.

[4] Lu, J., Du, H., Zhao, R., Li, H., Tan, Y., & Guo, W. (2024). Optimal Scheduling of the Active Distribution Network with Microgrids Considering Multi-Timescale Source-Load Forecasting. Electronics (2079-9292), 13(17).

[5] He, Y., Li, Z., Zhang, J., Shi, G., & Cao, W. (2023). Day-ahead and intraday multi-time scale microgrid scheduling based on light robustness and MPC. International Journal of Electrical Power & Energy Systems, 144, 108546.

[6] Yang, M., Cui, Y., Huang, D., Su, X., & Wu, G. (2022). Multi-time-scale coordinated optimal scheduling of integrated energy system considering frequency out-of-limit interval. International Journal of Electrical Power & Energy Systems, 141, 108268.

[7] Hou, J., Yu, W., Xu, Z., Ge, Q., Li, Z., & Meng, Y. (2023). Multi-time scale optimization scheduling of microgrid considering source and load uncertainty. Electric Power Systems Research, 216, 109037.

[8] Lai, Y., Zheng, W., Sun, Z., Zhou, Y., & Chen, Y. (2024). Micro-grid source-load storage energy minimization method based on improved competitive depth Q-network algorithm and digital twinning. Energy Informatics, 7(1), 126.

[9] Wang, X., Du, X., Wang, H., Yan, S., & Fan, T. (2024). Research on Coordinated Optimization of Source-Load-Storage Considering Renewable Energy and Load Similarity. Energies, 17(6), 1301.

[10] Qian, J., Guo, Y., Wu, D., Liu, A., Han, Z., Liu, Z., ... & Yang, X. (2024). Research on multi-time scale optimization of integrated energy system based on multiple energy storage. Journal of Energy Storage, 102, 113892.

[11] Deng, L., Chen, X., Dong, X., Liu, X., & Zhang, X. (2023, September). Collaborative Power Generation Scheduling of Source-Load Box-Type Substation Considering Uncontrollable Load. In 2023 3rd International Conference on Energy, Power and Electrical Engineering (EPEE) (pp. 168-173). IEEE.

[12] Jiang, P., Dong, J., & Zhu, Y. (2023). Mixed linear model of a safety dispatch model in an active distribution network for source–grid–load interactions. World Electric Vehicle Journal, 14(6), 159.

[13] Ma, H., Liu, Z., Li, M., Wang, B., Si, Y., Yang, Y., & Mohamed, M. A. (2021). A two-stage optimal scheduling method for active distribution networks considering uncertainty risk. Energy Reports, 7, 4633-4641.

[14] Guo, X., Li, Y., Wu, F., Shi, L., Chen, Y., & Wang, H. (2024). Optimal Battery Storage Configuration for High-Proportion Renewable Power Systems Considering Minimum Inertia Requirements. Sustainability, 16(17), 7830.

[15] Huang, Z., Liu, L., & Liu, J. (2023). Multi-time-scale coordinated optimum scheduling technique for a multi-source complementary power-generating system with uncertainty in the source-load. Energies, 16(7), 3020.

[16] Han, H., Wu, C., Wei, Z., Zang, H., Sun, G., Sun, K., & Wei, T. (2021). A two-stage cooperative dispatch model for power systems considering security and source-load interaction. Sustainability, 13(23), 13350.

[17] Li, G., Lin, X., Kong, L., Xia, W., & Yan, S. (2024). Enhanced bi-level optimal scheduling strategy for distribution network with multi-microgrids considering source-load uncertainties. Frontiers in Energy Research, 12, 1413935.

[18] Zhang, X., Zhang, M., Xu, L., Huang, R., & Li, C. (2024, July). Optimal allocation of offshore wind power and energy storage considering source-load power stochasticity. In Journal of Physics: Conference Series (Vol. 2806, No. 1, p. 012011). IOP Publishing.

[19] Tian, J., Zhang, Y., Gao, Y., Qin, Y., Fan, B., Zhang, C., & Zang, Q. (2024). Distributed optimization and scheduling strategy for source load storage distribution grid based on alliance chain. AIMS Energy, 12(5), 946-967.

[20] Huang, K., Fu, M., & Ding, X. (2023). Security and Economic Integration Scheduling of Electricity-Heat Integrated Energy System. IEEE Access, 11, 112236-112247.

[21] Qiu, H., Gu, W., Liu, P., Sun, Q., Wu, Z., & Lu, X. (2022). Application of two-stage robust optimization theory in power system scheduling under uncertainties: A review and perspective. Energy, 251, 123942.

[22] Wang, F., Zhou, L., Ren, H., Liu, X., Talari, S., Shafie-khah, M., & Catalao, J. P. (2017). Multi-objective optimization model of source–load–storage synergetic dispatch for a building energy management system based on TOU price demand response. IEEE Transactions on Industry Applications, 54(2), 1017-1028.

[23] Zeng, L., Gong, Y., Xiao, H., Chen, T., Gao, W., Liang, J., & Peng, S. (2024). Research on interval optimization of power system considering shared energy storage and demand response. Journal of Energy Storage, 86, 111273.

[24] Luo, H., Luo, L., Leng, Z., Hu, Y., & Yang, S. (2024, May). Aggregation frequency regulation strategy for wind and solar storage systems considering inertia adaptation. In Eighth International Conference on Energy System, Electricity, and Power (ESEP 2023) (Vol. 13159, pp. 688-694). SPIE.

[25] Meng, J., Deng, H., Yu, M., Yang, S., Tan, H., & Chen, H. (2024). A day-ahead coordinated scheduling strategy for source storage and load considering demand response and lines loss. Journal of Computational Methods in Science and Engineering, 24(1), 37-49.

[26] Zheng, S., Liao, K., Yang, J., & He, Z. (2022). Optimal scheduling of distribution network with autonomous microgrids: Frequency security constraints and uncertainties. IEEE Transactions on Sustainable Energy, 14(1), 613-629.

[27] Pang, K., Wang, C., Hatziargyriou, N. D., & Wen, F. (2023). Microgrid formation and real-time scheduling of active distribution networks considering source-load stochasticity. IEEE Transactions on Power Systems, 39(2), 2801-2813.

[28] Yan, K., Li, G., Zhang, R., Xu, Y., Jiang, T., & Li, X. (2023). Frequency control and optimal operation of low-inertia power systems with HVDC and renewable energy: A review. IEEE Transactions on Power Systems, 39(2), 4279-4295.

[29] Guo, T., Guo, Q., Huang, L., Guo, H., Lu, Y., & Tu, L. (2023). Microgrid source-network-load-storage master-slave game optimization method considering the energy storage overcharge/overdischarge risk. Energy, 282, 128897.

[30] Wang, C., Fu, S., Zhang, L., Jiang, Y., & Shu, Y. (2023). Optimal control of source–load–storage energy in DC microgrid based on the virtual energy storage system. Energy Reports, 9, 621-630.

[31] He, X., Ge, S., Liu, H., Xu, Z., Mi, Y., & Wang, C. (2023). Frequency regulation of multi-microgrid with shared energy storage based on deep reinforcement learning. Electric Power Systems Research, 214, 108962.

[32] Qizhen Wang & Gang Wang. (2025). Data-selective uniform probability density function for adaptive filtering. Digital Signal Processing104948-104948.

[33] Chunhui Ji,Guang Jin & Ran Zhang. (2025). State of charge estimation for lithium-ion batteries based on a digital twin hybrid model. Energy Reports2174-2185.

[34] Bingbiao Shi & Zhigao Chen. (2025). A study of distributed power access capacity taking into account distribution network state analysis. Journal of Physics: Conference Series(1),012008-012008.